Electron stimulated desorption from PF3 adsorbed on Pt. I. Positive ions

M. Akbulut, T. E. Madey, L. Parenteau, and L. Sanche

Citation: The Journal of Chemical Physics **105**, 6032 (1996); doi: 10.1063/1.472439
View online: http://dx.doi.org/10.1063/1.472439
View Table of Contents: http://scitation.aip.org/content/aip/journal/jcp/105/14?ver=pdfcov
Published by the AIP Publishing

Electron stimulated desorption from PF_3 adsorbed on Pt. I. Positive ions

M. Akbulut and T. E. Madey[a)]
Department of Physics and Astronomy and Laboratory for Surface Modification, Rutgers, The State University of New Jersey, Piscataway, New Jersey 08855

L. Parenteau and L. Sanche[a)]
Medical Research Council Group in Radiation Science, Faculté de Médicine, Université de Sherbrooke, Sherbrooke Quebec I1H 5N4, Canada

(Received 27 March 1996; accepted 2 July 1996)

We have studied electron stimulated desorption (ESD) of positive ions from PF_3 molecules adsorbed on a Pt substrate over a wide electron energy range (0–175 eV). Electron bombardment of 1 ML PF_3 adsorbed on the Pt surface gives rise mainly to an F^+ signal, whereas ESD from 6 ML thick PF_3 film (thick PF_3 layer) leads to P^+, PF^+, and PF_2^+ signals, in addition to F^+. We find that the onset for F^+ desorption from the 1-ML PF_3/Pt is at ~26.5 eV, while the F^+ threshold from the thick PF_3 layer is ~28.5 eV. The P^+ appearance potential from the thick PF_3 layer is ~23 eV. The ESD F^+ ion energy distribution has a peak energy of ~4 eV for all electron impact energies and a full width at half maximum (FWHM) of ~3 eV. The P^+ ions desorb with a peak energy of ~2 eV under 55 eV electron impact; the FWHM of the P^+ energy distribution is ~2 eV. We suggest that the near threshold P^+ formation from PF_3 corresponds to the excitations of the $6a_1$ level, while the F^+ threshold for adsorbed PF_3 on the Pt surface is due to the excitation of the F $2s$ level. Our results suggest that beyond near threshold (>32 eV), the excitation of the F $2s$ level also contributes significantly to the formation of P^+ and PF^+ ions from adsorbed PF_3. © *1996 American Institute of Physics.* [S0021-9606(96)01638-8]

I. INTRODUCTION

Electron stimulated desorption ion angular distribution (ESDIAD) measurements of F^+ and F^- ions from PF_3 adsorbed on various metal surfaces have been extensively studied in order to investigate the bonding mechanisms of adsorbed PF_3 (Refs. 1–5) as well as the coverage dependent azimuthal orientations of adsorbed PF_3.[6,7] When PF_3 bonds through the P atom to a surface atom, the P–F bonds are oriented away from the surface. Electron bombardment of adsorbed PF_3 results in desorption of both F^+ and F^- ions with high yields. ESDIAD imaging of adsorbed PF_3 by observation of F^- or F^+ ions has provided information about the azimuthal orientation and the polar angle of these bonds.[1,3,7–9] Although ESDIAD of halogen species from PF_3 adsorbed on metal surfaces have been the subject of various studies, mechanisms of electron stimulated desorption (ESD) from PF_3 (such as dissociative electron attachment and dipolar dissociation) leading to desorption of negative and positive ions have not been investigated. Even in the gas phase, mechanisms of ion formation from PF_3 have not been studied in detail.[10–12]

In this paper, we report on the ESD of F^+, P^+, and PF^+ ions from PF_3 molecules adsorbed on a Pt substrate over a wide electron energy range (0–175 eV). In the following paper[13] (hereafter paper II), we present the ESD of negative ions (F^-, F_2^-, and P^-) from PF_3 molecules adsorbed on a Pt substrate in the same electron energy range. The main motivation for these studies is to provide background information for a series of studies of the transmission of F^+, F^- ions through ultrathin films; in these experiments the transmission of F^+ and F^- ions produced by ESD from a saturation coverage of PF_3 on Ru(0001) has been studied through various atomic (such as Xe and Kr)[14,15] and molecular (such as H_2O) overlayer films.[16] In order to understand these results better, a knowledge of the ESD mechanisms of F^+ and F^- ions from adsorbed PF_3 is necessary.

A Pt substrate is used to study ESD mechanisms of positive and negative ions from PF_3. It has been shown that the bonding interaction of PF_3 with a Pt surface is similar to the bonding interaction of PF_3 with a Ru surface.[17] The bond formation of PF_3 with both Ru and Pt surfaces is believed to involve charge donation through the highest occupied molecular orbital (HOMO) of PF_3, and back charge donation into the lowest unoccupied molecular orbital (LUMO) of PF_3 (see Table II). PF_3 is bonded through the phosphorus atom to both Ru and Pt substrates. Therefore, we believe that the ESD mechanisms observed from a PF_3 covered Pt surface should be similar to those found for PF_3 adsorbed on Ru.

In this work, we find that ESD of 1 ML PF_3 adsorbed on the Pt surface gives rise mainly to an F^+ signal, whereas ESD from a 6 ML thick PF_3 film (thick PF_3 layer) leads to P^+, PF^+, and PF_{2+} signals, in addition to F^+. The onset for F^+ desorption from the 1 ML PF_3/Pt is at ~26.5 eV, while the F^+ threshold energy from the thick PF_3 layer (6 ML PF_3 on Pt) is ~28.5 eV. The threshold energy for P^+ formation from PF_3 is ~23 eV. Within the 40–175 eV incident electron energy range, the ESD F^+ ions have a peak kinetic energy of ~4 eV and the full width at half maximum of the F^+ energy distribution is ~3 eV. The P^+ ions desorb with a peak energy of ~2 eV under 55 eV electron bombardment.

This paper is organized as follows. In the next section,

[a)]Authors to whom correspondence should be addressed.

 0021-9606/96/105(14)/6032/11/$10.00

we describe the experimental details. In Sec. III, we present the ESD measurements from a saturation coverage of PF_3 on Pt (1 ML PF_3/Pt surface) and a thick PF_3 layer on Pt (6 ML PF_3/Pt surface). In Sec. IV, we discuss the results, and finally in Sec. V we provide a summary.

II. EXPERIMENTAL SETUP

The experiments are performed in Sherbrooke using an ultra high vacuum (UHV) chamber reaching a base pressure $\sim 1\times 10^{-10}$ Torr as described elsewhere.[18–20] The apparatus consists of a polycrystalline Pt foil press-fitted directly onto the cold tip ($\sim$17 K) of a closed-cycle refrigerated cryostat which is bombarded by an electron beam from an electron monochromator in order to initiate ESD of ions from films condensed on the Pt surface; a quadrupole mass spectrometer (QMS) detects a large portion of the ESD ion flux desorbing from the surface. The entire experimental assembly is enveloped by a double μ-metal shield in order to reduce stray magnetic fields in the monochromator and at the surface. The Pt sample is cleaned by resistive heating at $\sim$1000 K. After heating the sample at $\sim$1000 K, no ESD signal from the sample is detected by the QMS.

The electron source is a custom-designed hemispherical electron monochromator,[21] with a central trajectory radius of 2.5 cm and an operational pass energy of $\sim$3.5 eV. The electron beam energy has a full width at half maximum (FWHM) of 80 meV. The absolute energy scale of the incident electron beam is determined to within $\pm$0.15 eV of the vacuum level ($E_{vac}=0$ eV) by observing the onset of current transmission to the Pt sample as a function of electron energy.[21,22]

The output lens, which focuses the beam on the target, consists of a double-zoom electrostatic system that enables us to maintain a relatively constant incident current vs electron energy across a given energy region (i.e., 2–20 eV, 20–175 eV). The angle of incidence for the electron beam is 70° from the surface normal. The electron beam current, as measured at the target, is about 5 nA. The electron beam has a spatial width of about 0.2 cm. The portion of the target illuminated by the incident electron beam has an elliptical shape of 0.1 cm^2 area.

The QMS is positioned at 20° from the surface normal.[23,24] The acceptance angle of the ion optics, preceding the QMS, is about 25°. Two grids are positioned at the entrance of the mass spectrometer, which permit measurement of the ion kinetic energy distributions by application of a retarding potential (V_r). The QMS can be operated in two modes: (a) the ion yield mode and (b) the ion kinetic energy mode. In the ion yield mode, ions of selected mass are detected as a function of incident electron energy. In the ion kinetic energy mode, the ion current at a selected mass is measured for a fixed incident electron energy as a function of the retarding potential.

III. RESULTS

ESD positive ion mass spectra from 1 ML of PF_3 and 6 ML of PF_3 on the Pt surface at an electron energy of 56 eV are presented in Figs. 1(a) and 1(b), respectively. As seen in Fig. 1(a) for the 1 ML PF_3/Pt surface, ESD of PF_3 results in a large F^+ signal and a small P^+ signal; the F^+ signal is $\sim$4 times larger than the P^+ signal. However, ESD from the 6 ML thick PF_3 film on the Pt surface leads to appearance of PF^+ and $(PF_2)^+$ signals, in addition to the F^+ and P^+ signals.

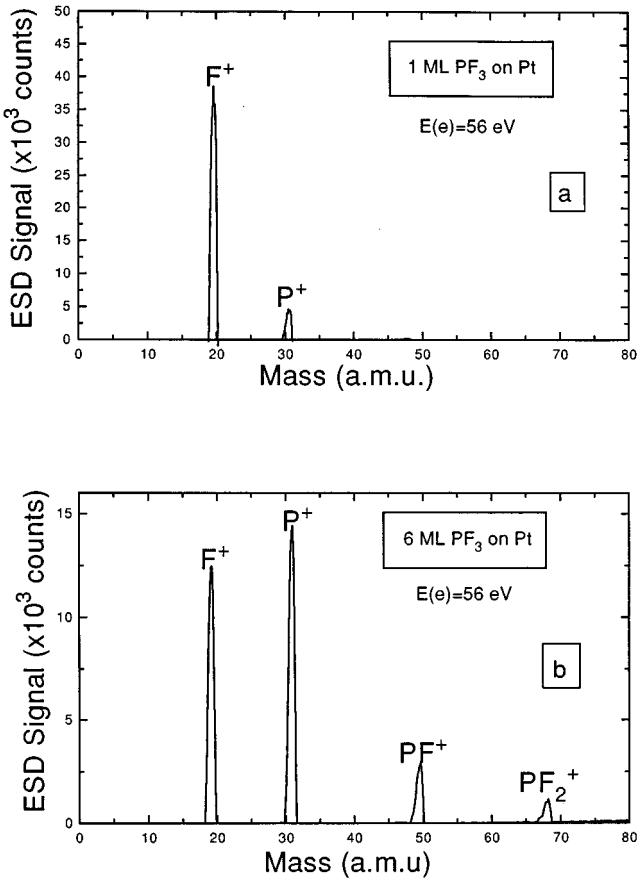

FIG. 1. Electron stimulated desorption (ESD) positive ion mass spectra from (a) 1 monolayer (ML) of PF_3 on the Pt surface and (b) a thick (6 ML) PF_3 layer on the Pt surface.

Figure 2 shows the F^+ and P^+ intensities as a function of PF_3 film thickness on the Pt surface at an electron energy of $\sim$60 eV. The F^+ ESD intensity rises very steeply, reaches a maximum at around 1 ML, decreases to $\sim$40% of the maximum F^+ value at around 5 ML, and then remains constant with increasing PF_3 thickness. In contrast, the P^+ intensity increases with PF_3 thickness to a saturation value at around 5 ML.

Since PF_3 is condensed on the Pt surface at $\sim$17 K we do not expect that PF_3 forms three-dimensional clusters upon adsorption at $\sim$17 K; PF_3 grows statistically and forms amorphous solid PF_3. Indeed, our ESD results (Fig. 2) support this: ESD yields from adsorbed PF_3 layers thicker than 5 ML are independent of thickness. This indicates that the ESD ions from the 6 ML PF_3 surface originate mainly from the top few layers. This is consistent with Refs. 13–15, in which it has shown that some low energy ions created *below the surface layer* can penetrate several layers and contribute to ESD ion signal.

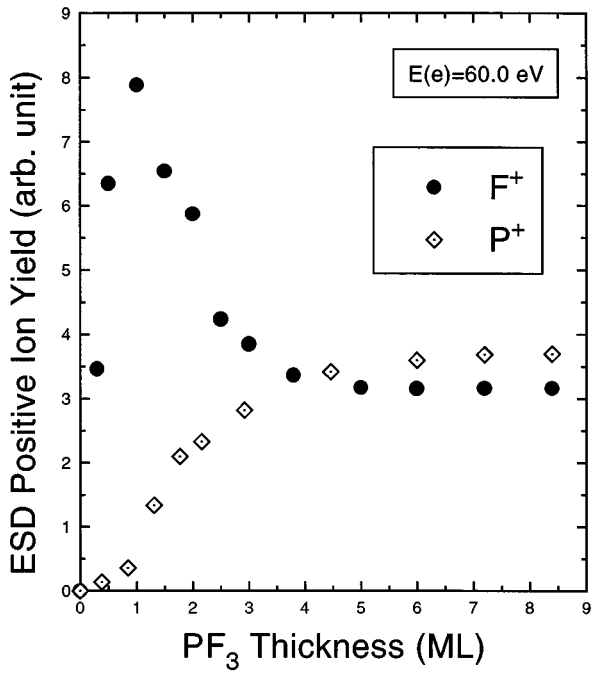

FIG. 2. F^+ and P^+ ESD yields as a function of PF_3 thickness.

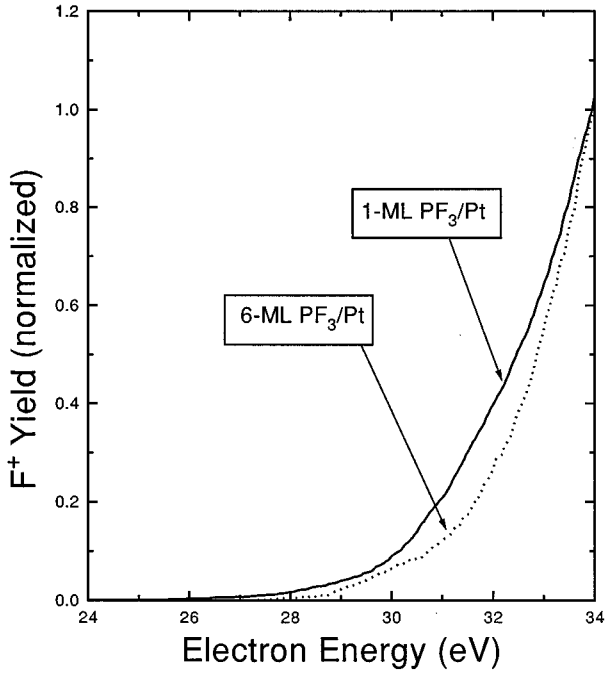

FIG. 3. F^+ ESD yield functions obtained from 1 ML PF_3/Pt and 6 ML PF_3/Pt surfaces in the electron energy range 24–36 eV. Note, that the F^+ yields are normalized to the 34 eV intensity: The F^+ yield intensity at 34 eV obtained from 1 ML PF_3/Pt surface is ~5 times larger than from obtained from 6 ML PF_3/Pt surface.

In the following, we present the F^+, P^+, and PF^+ ion yields as a function of primary electron energy and the kinetic energy distributions of F^+ and P^+ ions from PF_3 adsorbed on Pt.

A. F^+ from PF_3 on Pt

In Fig. 3, the normalized F^+ yield curves from the 1 ML PF_3/Pt and 6/ML PF_3/Pt surfaces are shown in the electron energy range of 24–34 eV. In order to compare the shape of the F^+ yield curves near threshold, they are normalized to unity at 34 eV. It can be seen that the slope of the F^+ yield from the 1 ML PF_3/Pt surface is different from that of the F^+ yield from the 6 ML PF_3/Pt. As seen in Fig. 3, the F^+ ESD yield obtained from the 1 ML PF_3/Pt surface has an onset at ~26.5 eV, whereas the F^+ energy threshold from the thick PF_3 (6 ML PF_3/Pt surface) is ~28 eV; the F^+ threshold energy from absorbed PF_3 depends on the PF_3 film thickness.

An F^+ ESD yield curve obtained from the 1 ML PF_3/Pt surface is shown in Fig. 4 as a function of electron energy in the range 0–170 eV. At electron energies above ~30 eV, the F^+ yield increases almost linearly with increasing electron energy up to ~100 eV and then increases with diminishing slope up to 170 eV.

In order to determine the F^+ kinetic energy distribution, the F^+ ESD signal is monitored as the retardation potential, V_r, is scanned over a suitable range. The kinetic energy distribution of the F^+ ions is obtained by taking the negative derivative of the retardation curve with respect to V_r. Figure 5 shows normalized kinetic energy distributions of the F^+ ions from a 1 ML PF_3/Pt surface obtained with incident electron energies of 40, 55, 125, and 175 eV. The most probable kinetic energy (peak energy) of the F^+ ions is ~4 eV. The most probable kinetic energy of the F^+ ions does not depend on electron energy, within experimental uncertainty.

The kinetic energy distributions of the F^+ ions obtained from the 1 ML PF_3/Pt and 6 ML PF_3/Pt surfaces for an incident electron energy of 55 eV are shown in Fig. 6. It can

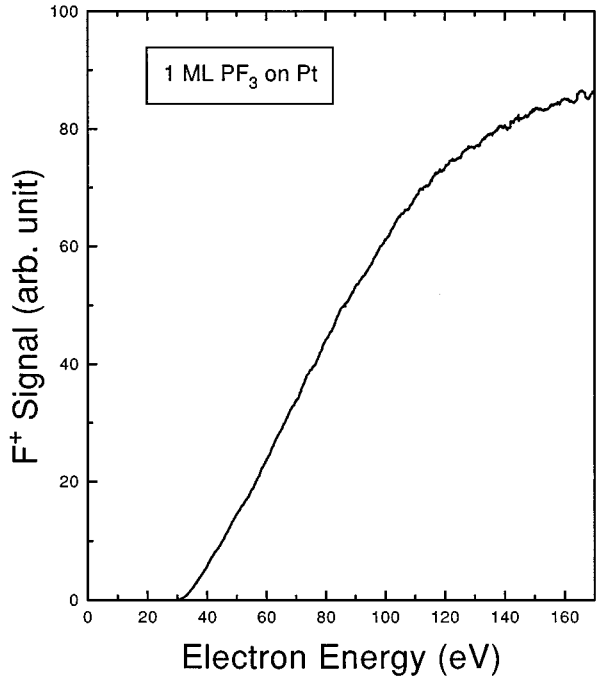

FIG. 4. F^+ ESD yield curve obtained from 1 ML PF_3/Pt surface as a function of electron energy in the range of 0–175 eV.

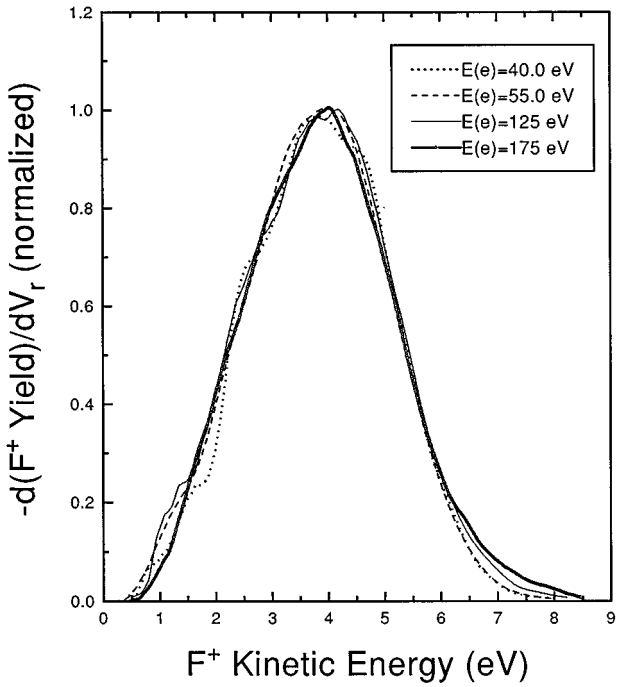

FIG. 5. Kinetic energy distributions of the F^+ ions from a 1 ML PF_3/Pt surface obtained with incident electron energies of 40, 55, 125, and 175 eV. Yields are normalized to unity at their maximum.

be seen that the F^+ distribution for the 6 ML PF_3/Pt surface is slightly different from the F^+ distribution for the 1 ML PF_3/Pt surface. Based on these and similar measurements, we conclude that the full width at half maximum (FWHM) of

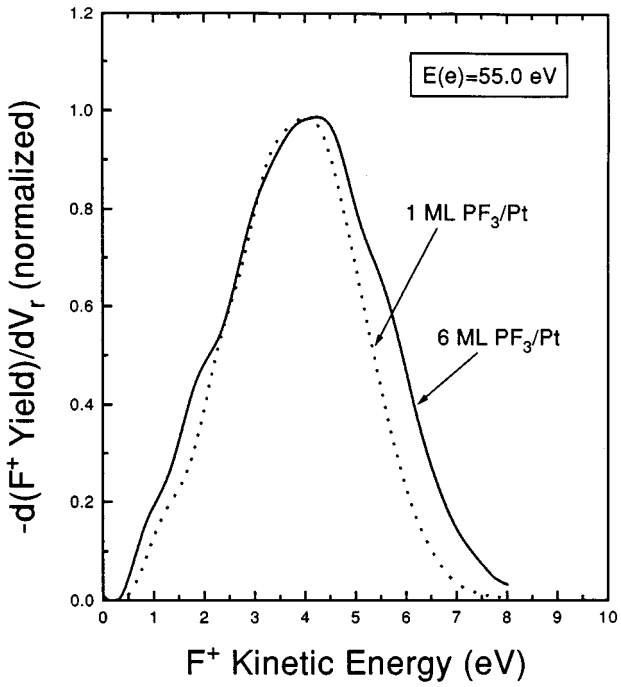

FIG. 6. Comparison of the kinetic energy distribution of the F^+ ions from 1 ML of PF_3 on the Pt surface with the kinetic energy distribution of the F^+ ions from 6 ML of PF_3 on the Pt surface for an incident electron energy of 55 eV. Yields are normalized to unity at their maximum.

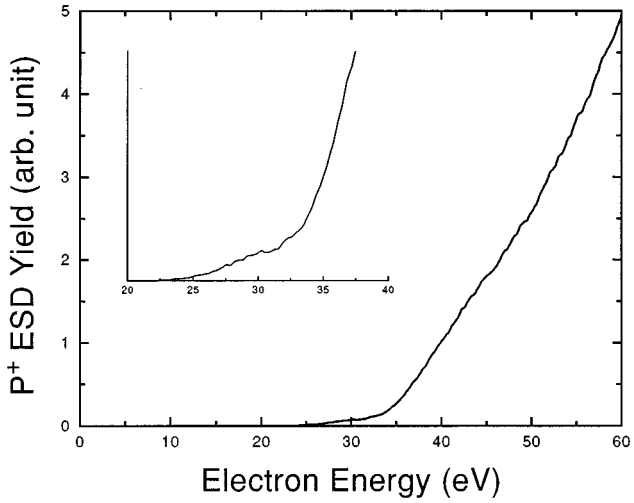

FIG. 7. P^+ ESD yield curve obtained from 6 ML PF_3/Pt surface as a function of electron energy in the range of 0–60 eV. The threshold region is shown on an extended scale in the inset.

the F^+ kinetic energy distribution increases and the peak energy shifts to higher energy with increasing PF_3 thickness up to 5 ML.

B. P^+ from PF_3 on Pt

Figure 7 shows the electron energy dependence of the P^+ signal from the thick PF_3 film in the range 0–60 eV. As seen in the inset of Fig. 7, the P^+ ESD yield from the thick PF_3 film has an onset at ~23 eV. The P^+ signal increases slowly between 23 and 32 eV, and then increases steeply with increasing electron energy.

The kinetic energy distribution of the P^+ ions from the thick PF_3 film on Pt for an incident electron energy of 55 eV is shown in Fig. 8. The P^+ ions desorb with a peak energy of ~2 eV; the full width at half maximum (FWHM) of the energy distribution of the P^+ ions from the 6 ML PF_3/Pt surface is ~2 eV.

C. PF^+ from PF_3 on Pt

In Fig. 9, the F^+, P^+, and PF^+ yield curves from the thick PF_3 film are compared in the electron energy range 20–40 eV, so that we compare thresholds on similar intensity scales. Note, that the ion yields in Fig. 9 are normalized to unity at 40 eV. The threshold energy for the PF^+ formation from the adsorbed PF_3 is $\sim 25 \pm 1$ eV. Since the PF^+ yield is very low (cf. Fig. 1), the PF^+ kinetic energy distribution cannot be measured reliably.

Although the low energy thresholds differ for the three ions, both P^+ and PF^+ yield curves exhibit significant changes in slopes above ~33 eV, the region of the F^+ threshold. The similarity between the yield curves above ~33 eV suggests that F^+, P^+, and PF^+ formation above ~33 eV from the thick PF_3 on Pt may be initiated by the excitation of the F 2*s* level and/or multivalence excitations (e.g., 2h, 2h1e), as discussed in Secs. IV B and IV D.

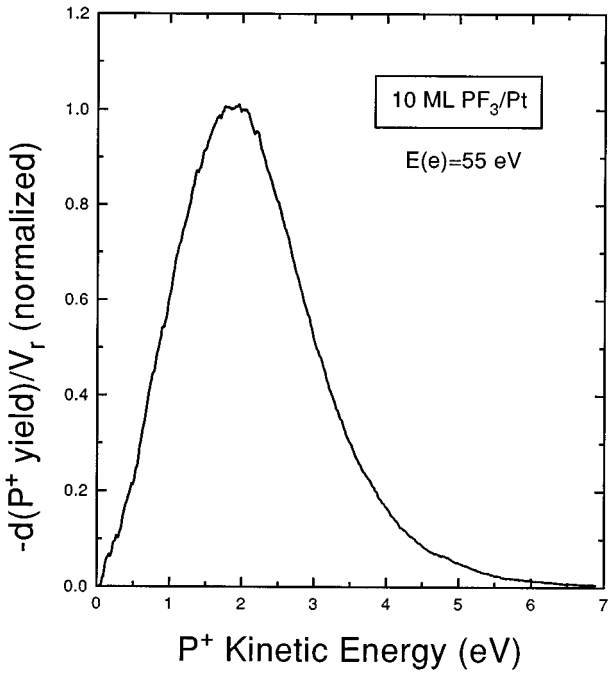

FIG. 8. Kinetic energy distributions of the P^+ ions from a 6 ML PF_3/Pt surface obtained with incident electron energies of 55 eV.

IV. DISCUSSION

Above a certain energy threshold, electrons impinging on surfaces containing either adsorbed atomic or molecular layers, or terminal bulk atoms, can induce electronic transitions to states that are repulsive in character, and the subsequent conversion of potential energy into motion of the excited species can result in the emission of particles (such as positive ions, negative ions or metastables) from the surface. ESD positive ion emission is generally initiated by valence or core excitation processes.[25–27] The threshold energy for desorption of positive ions can be as low as 15 eV; this correlates with a valence excitation of the adsorbate. Valence excitations of adsorbed molecules by electron impact may lead to desorption of positive ions via dissociative ionization or dipolar dissociation (DD).[23,24,28] DD (or ion pair formation) occurs when an incident electron excites a valence electron of a target molecule into a highly excited neutral intermediate state which dissociates into positive and negative ion fragments.

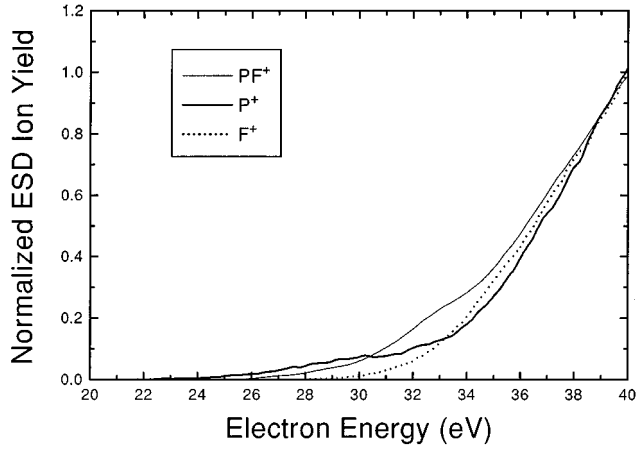

FIG. 9. F^+, P^+, PF^+ ESD yield curves obtained from 6 ML PF_3/Pt surface as a function of electron energy in the range of 20–40 eV. The ion yields are normalized to unity at 40 eV in order to compare the shapes of the ion yield functions. Note, that the ratio of P^+:F^+:PF^+ intensities at 40 eV are ~5:4:1.

Recent experimental and theoretical studies on ESD from adsorbed molecules (e.g., N_2, CO, H_2O, $C_6H_{11}F$, and C_6H_{12}) have shown the importance of 2-hole (2h) or 2-hole 1-electron (2h1e) ''multiexcited'' valence states in initiating the desorption of positive ions from surfaces.[29–35] Recent photodissociation studies on small molecules such as N_2, CO, and H_2O, have revealed that the multi-excited states appear as satellites in photoelectron spectra.[34,36]

In ionic and covalent systems, the desorption of ions may be initiated by the ionization of a core level; this can be explained in the context of the Auger stimulated desorption (ASD) model.[26,36] The ASD model is based on the creation of a core hole as the primary process, followed by an Auger decay. That produces an electronic state with multiple holes (2h, 3h). In ionic systems, the interatomic Auger decay of the core-hole creates a positive ion at an initially negative ion site, and repulsive Coulomb interactions resulting from the reversal of the Madelung potential provide the driving force for positive ion desorption (the Knotek–Feibelman model).[37] On the other hand, in covalent systems, if the holes are localized for a sufficiently long time in a bonding orbital, the hole–hole repulsion can result in the desorption of a positive ion.[34,36]

In the presence of a polarizable medium such as a metal surface, and/or a molecular solid, the energetics of the ESD processes leading to the desorption of ions from an adsorbed molecule can be different from the ion formation processes for the same molecule the gas phase.[23,38] The image potential in a metal and/or the induced polarization force within a molecular solid can affect the initial and final ESD processes. The influence of the image force on the initial ESD process depends strongly on the nature of the dissociative excited states. It has been shown that the polarization energy of the medium (a molecular solid and/or a metal surface) can reduce the energy of the dissociative valence states (ionic) with respect to the neutral state.[23,28] Following a dissociation process that leads to formation of an ion, the image potential also acts on the desorbing ion by lowering its desorbing energy (the final state effect). Depending on the strength of bonding of the molecule to substrate, the manifold of final states can be substantially different from that of the free molecule.[23,28] In addition, the presence of a surface can also result in charge transfer neutralization processes that dramatically affect ESD yields.[25,28,36]

The ion desorption thresholds and kinetic energies provide insights into processes involved in the ion desorption. Comparison of the ion desorption thresholds and kinetic energies with experimental gas phase data and calculated excited state potential energy curves are therefore, extremely useful in identifying ESD mechanisms for ion desorption

TABLE I. Ground state valence orbitals in PF_3 (Ref. 40).

		Electronic populations							
		P				F			
Orbital	Energy (eV)	3*s*	4*s*	3*p*	4*d*	2*s*	3*s*	2*p*	3*p*
$6a_1$	−16.37	0.35				0.23	0.01	0.40	0.01
$4e$	−13.42			0.16	0.01	0.06	0.01	0.76	
$7a_1$	−12.92	0.06		0.14	0.02	0.01		0.77	
$5e$	−11.61				0.02			0.97	
$6e$	−10.55				0.01			0.99	
$1a_2$	−10.14							0.99	
$8a_1$	−7.90	0.29		0.32	0.01		0.01	0.36	
$7e$	−1.05			0.44	0.23	0.04	0.03	0.26	
$9a_1$	+1.94		0.12	0.24		0.08	0.33	0.21	0.01
$10a_1$	+4.74	0.04	0.13	0.09	0.01	0.02	0.52	0.10	0.02

from species adsorbed on the surface. However, potential energy curves of PF_3 are not known; they have neither been measured nor calculated. Therefore, in the following discussion, the possible ESD mechanisms that may lead to desorption of positive ions from adsorbed PF_3 are based only on energetic considerations.

In the next Sec. (IV A), we first discuss the positive ion yields as a function of PF_3 film thickness, and in Secs. IV A–IV D we discuss the possible ESD positive ion desorption mechanisms in the near-threshold region.

A. F^+ and P^+ yields as a function of PF_3 thickness

It is likely that the decrease in the F^+ signal and the increase in the P^+ signal for >1 ML (Fig. 2) are due to a change in the orientation of PF_3 molecules. In the first monolayer, the PF_3 molecules are expected to bond through the P atoms to the Pt surface, and the P–F bonds are oriented away from the surface.[1,2,7,8,39] ESD from the 1 ML PF_3/Pt surface leads mainly to the desorption of F^+ ions. However, for >1 ML the PF_3 molecules are expected to orient randomly, because of the weak PF_3–PF_3 interaction.[39] This may result in a decrease in the F^+ ESD signal from a thick PF_3 layer, and an increase in the P^+ signal.

As shown in paper II,[13] the PF_3 thickness dependence of the F^- yields produced via a dissociative electron attachment (DEA) process is different from the F^- yields produced via a dipolar dissociation (DD) process. The DEA F^- intensity increases with PF_3 film thickness to a saturation value at ~ 5 ML, while the DD F^- intensity decreases for >1 ML and reaches a saturation value at ~ 7 ML. As we discuss extensively paper II,[13] the changes in the F^- intensities as a function of PF_3 film thickness are mainly caused by the image potential induced in the Pt surface, which affects the DEA F^- and DD F^- yields differently. Since the F^+ yield is different from the P^+ as a function of PF_3 film thickness, and neither DEA nor DD processes lead to desorption of positive ions from adsorbed PF_3 (see next sections), we do not consider that image potential effects have an important influence on the positive ion yields for >1 ML.

A striking observation is that from the thick PF_3 film the P^+ signal is ~ 1.2 times larger than the F^+ signal [Figs. 1(b) and 2]. This observation is in excellent agreement with the cracking pattern of P^+ and F^+ from PF_3 at 70 eV in the gas phase.[12] The similarity of results from the thick PF_3 layer and from the gas phase suggest that the electronic structure (orbital energies) of the PF_3 molecule remain essentially unchanged in going from the gas phase to condensed phase, and that the manifold of excited states that lead to dissociation and their relative lifetimes are not considerably affected.

B. Mechanisms of ESD of F^+ from adsorbed PF_3

In a gas phase experiment, the threshold energy leading to F^+ formation from PF_3 has been found to be ~ 36 eV;[12] to explain the F^+ formation from PF_3, the reaction

$$e^- + PF_3 \rightarrow P + 2F + F^+ + 2e^-, \tag{1}$$

has been suggested[12] based only on a thermodynamic argument. The calculated appearance potential for zero kinetic energy F^+ generated via reaction (1) is ~ 32.7 eV. The gas phase F^+ threshold energy (~ 36 eV) from PF_3 is comparable to the F 2*s* ionization energy (~ 34–39 eV) of PF_3 (see Table III). It is reasonable to suggest that the F^+ formation in the gas phase could involve excitation from or ionization of the F 2*s* orbital in PF_3. Moreover, when PF_3 is adsorbed on a metal surface the threshold energy leading to F^+ formation from PF_3 can be lower than that of the gas phase, because an electronic transition from the PF_3 core level to the substrate Fermi level is possible and also because of the polarization energy of PF_3^+.

At this point, it is helpful to consider the electronic structure and one-electron valence ionization potentials of PF_3. In Table I, we list valence orbitals and their electronic populations for PF_3.[40] The ground state valence orbitals in PF_3 listed in Table I have been calculated using the self-consistent multipolar (SCM) method.[40] The highest occupied molecular orbital (HOMO) of PF_3 is the $8a_1$ orbital; this orbital is a lone pair orbital consisting primarily of phosphorous 3*p* and 3*s* atomic orbitals. The lowest unoccupied molecular orbital (LUMO) is the $7e$ antibonding orbital which consists primarily of *p* and *d* orbitals on the phosphorous atom. Experimental studies have shown that the bonding mechanism of PF_3 to metal surfaces is very similar to the

bonding of CO to metals:[16] the bond formation of PF_3 with a metal surface involves σ donation through the HOMO $8a_1$ to d vacancies on the surface metal atoms, and π-back donation from d orbitals into the LUMO $7e$.

The valence ionization energies of chemisorbed PF_3 with respect to Fermi levels of Ru(0001) and Pt(111) are listed in Table II.[17,41] Table III lists relative one-electron valence ionization potentials of free PF_3 and chemisorbed PF_3 on Ru(0001) and Pt(111) surfaces with respect to an internal reference $(6e+1a_2)$.[17,41] Note, that the ionization potentials of PF_3 adsorbed on the metal surface are referenced to the vacuum level which has to be displaced from the Fermi level by about 7.5 eV in order to line up the most intense peaks in the gas phase and the chemisorbed phase. Taking the work function of 1 ML PF_3/Pt to be ~5.5 eV,[17,42] we estimate the substrate induced ionization energy shift (relaxation energy, polarization energy, etc.) to be 2.0 eV. As seen in Table II, the ionization potential of the $8a_1$ orbital of PF_3 on the metal surfaces increases significantly upon adsorption, while the relative ionization potentials of the other orbitals of PF_3 are not affected significantly. There are no gas phase data available for the F $2s$ ionization potential from PF_3. However, we expect that the relative binding energy of the shallow core F $2s$ orbital remains almost unchanged on the metal surfaces.

In the following, we discuss the possibility of F^+ formation via valence-level excitation (including dissociative ionization and dipolar dissociation) as well as core-level excitation.

1. One-electron valence ionization

Ionization of gas phase PF_3 in the Franck–Condon regime could result in the formation of F^+, provided that ionic states are repulsive in character. In the gas phase, the ionization energies for the low-lying orbitals (spanning the range from the $8a_1$ orbital to the $6a_1$ orbital) are all lower than 23 eV (see Table III). This indicates that ionization of PF_3 by removing one electron from a low-lying orbital $(8a_1-6a_1)$ does not result in F^+ formation, because the gas phase F^+ threshold energy (~36 eV) from PF_3 is considerably larger than the ionization energies of these orbitals.

Consider now the possibility of F^+ formation from *adsorbed* PF_3 via valence-level ionization. As seen in Fig. 3, the ESD F^+ threshold energies obtained from the 1 ML PF_3/Pt and thick PF_3/Pt surfaces are ~26.5 and ~28.5 eV, respectively. Near the Pt surface, we expect that an initial excitation from a PF_3 valence or core orbital to the Fermi level of the substrate is the most likely excitation channel, because the Fermi level of the substrate is below the LUMO orbital energy of PF_3. Since the F^+ threshold energy from the 1 ML PF_3/Pt surface is ~26.5 eV and the ionization energies for the orbitals spanning the range from $8a_1$ orbital to the $6a_1$ orbital are lower than 16 eV with respect to the Fermi level of the substrate (see Table II), it is not energetically possible that only a one electron excitation from the orbitals between the $8a_1$ and the $6a_1$ to the Fermi level of the Pt substrate contributes to the formation of F^+ from PF_3 on the Pt surface.

2. Dipolar dissociation

We consider now the possibility that the near threshold F^+ production from PF_3 may be initiated via dipolar dissociation (DD). As we discuss in detail in the following paper,[13] DD (or ion pair formation) is the most important process leading to ESD of *negative ions* at electron energies above approximately 15 eV. In a DD process, for $E(e)>15$ eV a molecule may be excited to an electronically excited neutral intermediate state which dissociates spontaneously into a positive and negative ion fragment. This excitation leading to the ion pair formation may involve a single valence or a multivalence excitation of the molecule (such as 1-hole 1-electron, 2-hole 2-electron excitation). Some plausible DD reactions which could lead to the formation of F^+ ion from PF_3 by electron impact are

$$e^- + PF_3 \rightarrow [PF_3]^* + e^- \rightarrow [PF_2]^- + F^+ + e^-, \quad (2)$$

$$e^- + PF_3 \rightarrow [PF_3]^* + e^- \rightarrow F^- + F^+ + PF + e^-, \quad (3)$$

$$e^- + PF_3 \rightarrow [PF_3]^* + e^- \rightarrow [PF]^- + F^+ + F + e^-, \quad (4)$$

$$e^- + PF_3 \rightarrow [PF_3]^* + e^- \rightarrow F^- + F^+ + F + P + e^-, \quad (5)$$

$$e^- + PF_3 \rightarrow [PF_3]^* + e^- \rightarrow P^- + F^+ + 2F + e^-. \quad (6)$$

In the gas phase, the thermodynamic threshold energies (for zero eV kinetic energy F^+) for these reactions are 22.6, 23.8, 26.1, 28.4, and 31 eV, respectively.[43] Since DD involves an electronic transition from the ground state to a dissociative state, a $PF_3 \rightarrow [PF_3]^*$ transition leading to the formation of F^+

TABLE II. Ionization energies of chemisorbed PF_3 with respect to the Fermi level of the metal ($E_F=0$) (Ref. 17).

		Ionization potentials (eV)	
Orbital	Peak	PF_3/Ru(0001)	PF_3/Pt(111)
$8a_1$	a	6.25	7.7
$6e+1a_2$	b	8.65	9.2
$5e$	c	9.90	10.45
$(7a_1)+4e$	d	11.90	12.65
$6a_1$	e	15.15	15.85
F $2s$ (shallow core)		27–31[a]	

[a]Reference 41.

TABLE III. Relative ionization potentials of chemisorbed PF_3 with respect to an internal reference $(6e+1a_2$, F-lone pairs) (Ref. 17). Note, that the factor of 7.5 eV is used to line up the $(6e+1a_2)$ peaks in the gas phase and the chemisorbed phase.

	Ionization potentials (eV)			
Orbital	PF_3 (free)	PF_3/Ru(0001)	PF_3/Pt(111)	Peak
$8a_1$	12.27	13.75	14.60	a
$6e+1a_2$	16.10	16.10	16.10	b
$5e$	17.46	17.40	17.40	c
$7a_1$	18.60			
$4e$	19.50	19.40	19.55	d
$6a_1$	22.55	22.60	22.75	e
F $2s$ (shallow core)		34–39[a]		

[a]Reference 41.

via DD requires few eV more energy than the thermodynamic threshold energy. Therefore, in the Franck–Condon region, reactions (2)–(6) seems to be energetically possible pathways to produce F^+ ion from PF_3 in the gas phase. It can be seen in Table III that the one-electron ionization energies for the low-lying orbitals (spanning the range from the $8a_1$ orbital to the $6a_1$ orbital) are lower than 23 eV in the gas phase (and condensed phase), and 14.6 eV for 1 ML PF_3 on Pt. This indicates that one-electron transitions from the valence orbital ($8a_1$–$6a_1$) of PF_3 do not result in F^+ formation via DD, because the threshold energies of reactions (2)–(6) are larger than the ionization energies of these orbitals in the gas phase and near the Pt surface.

Similarly, since the P^+ and PF^+ threshold energies (~23 and ~25 eV, respectively) from the thick PF_3 films are larger than the ionization energies of the low-lying valence orbitals ($8a_1$–$6a_1$) of PF_3, we do not consider that DD leads to the P^+ and PF^+ formation from the thick PF_3 layer.

3. Multiple valence excitation: 2-hole or 2-hole 1-electron excitations

Since we have excluded dipolar dissociation and one-electron excitations from low-lying valence orbitals of PF_3 as possible mechanisms leading to the formation of F^+, we now consider other multi-electron excitation processes, such as 2h and 2h1e, that may result in F^+ formation from PF_3. It has been shown that 2h1e excitations derive their intensity from such processes as correlation mixing with a deep valence (shallow core) state or a core state at higher binding energy. If the effective hole–hole repulsion is greater than some appropriate covalent interaction, the repulsive multiexcited state is expected to be sufficiently long lived to lead to desorption of positive ions from surfaces.[26,36,44] In the UPS spectra for a wide range of molecules (such as CO and H_2O), the features (satellites) in the shallow core (deep valence) regions are attributed to the 2h1e excitations.[34–36] Therefore, we expect that there are some valence 2h1e states mixed with the $(F\ 2s)^{-1}$ state.

Near the Pt surface, assuming an initial electronic transition (one-electron transition) from PF_3 to the substrate Fermi level, the minimum energies required to create various 2h1e states are estimated to be ~28.0 eV for $(6a_1^{-1}6e^{-1}7e)$, ~26.1 eV for $(4e^{-1}5e^{-1}7e)$, and ~24.9 eV for $(5e^{-2}7e)$. However, in the solid PF_3, the minimum energies required to form various states are estimated to be ~35.2 eV for $(6a_1^{-1}6e^{-1}7e)$, ~33.6 eV for $(4e^{-1}5e^{-1}7e)$, and ~32.2 eV for $(5e^{-2}7e)$. (Note, that we assume that in solid PF_3 in order to create an $1h$ state an electron is ejected from PF_3 to vacuum.) This simple energy argument indicates that the 2h1e valence excitations near the Pt surface may initiate F^+ formation from adsorbed PF_3, whereas for the thick PF_3 film these excitations are not important processes for the near threshold F^+ desorption, because the excitation energies of these states lie well above the near threshold energy of ~29 eV for F^+ from the thick PF_3 film on the Pt surface. However, at higher energies (>32 eV), these excitations may be important; as seen in Fig. 3, the F^+ yield from the thick PF_3 film increases steeply above 32 eV.

4. Core-level excitation

As mentioned earlier, the F^+ threshold energy (~36 eV) from gaseous PF_3 is comparable to the F $2s$ ionization energy (34–39 eV); now, consider the possibility that the removal of an F $2s$ electron, which creates an $(F\ 2s)^{-1}$ core-hole state, may initiate the formation of F^+ from PF_3 in the gas phase. Since the F $2s$ orbital of PF_3 is characterized as a shallow-core orbital, the $(F\ 2s)^{-1}$ core-hole state is not expected to be repulsive. However, the $(F\ 2s)^{-1}$ state may decay via an Auger process to form a repulsive 2h state, or the $(F\ 2s)^{-1}$ state may cross a highly repulsive 2h1e (or 2h) state and predissociate. These processes following the creation of the $(F\ 2s)^{-1}$ state may result in F^+ formation from PF_3.

Let us now focus on the possible contribution of the F $2s$ orbital of PF_3 to the F^+ formation near the Pt surface and in the condensed PF_3 films. Recent soft x-ray photoelectron spectroscopy (SXPS) studies on the adsorption of PF_3 on Ru(0001) surface have shown that the SXPS F $2s$ signal is very broad with a peak energy of ~31 eV with respect to the Fermi level of the Ru(0001) substrate;[41] the F $2s$ ionization region extends over the range 34–39 eV with respect to the vacuum level (27–32 eV with respect to the Fermi level). Since the F $2s$ ionization energy with respect to the vacuum level (~34–39 eV) is larger than the F^+ desorption threshold (~27–29 eV), it seems that a direct electron ejection from the F $2s$ level to the vacuum does not lead to the F^+ desorption from the 1 ML PF_3/Pt surface. However, it is possible that an initial excitation from the F $2s$ orbital to the substrate Fermi level or to an unoccupied level in PF_3, requiring an electron energy on the order of 27–29 eV, may lead to desorption of the F^+ ions.

Figure 10 illustrates schematically the possible electronic transitions from the F $2s$ level to unoccupied levels in PF_3 and the Pt substrate. The center of the antibonding $7e$ LUMO of chemisorbed PF_3 is expected to be at about ~3.5 eV above the Fermi level of the Pt substrate.[17] Near the Pt surface, an initial electronic transition from the F $2s$ level (interface F $2s$) to the Fermi level is expected to dominate, because the Fermi level is below the lowest unoccupied level ($7e$ orbital) of PF_3. For the 1 ML PF_3/Pt surface, the ionization of the interface F $2s$ level may proceed via an electron transition to the Fermi level of the Pt substrate. As seen in Table II, the excitation of an F $2s$ electron to the Fermi level would require a minimum energy of ~27 eV. This value is in very good agreement with the observed F^+ threshold energy from the 1 ML PF_3/Pt surface (Fig. 3). In fact, F^+ desorption via excitation of the F $2s$ levels of adsorbed fluorine or adsorbed species containing fluorine on metal surfaces has been identified previously.[45,46] Recent experimental studies have revealed that F^+ formation from adsorbed fluorine on Si surfaces results from excitation of an F $2s$ electron to the Fermi level or Si conduction band minimum (CBM).[45–47]

As discussed in Refs. 9–11, some ions created below the surface can penetrate atomic or molecular films several layers thick. Although the majority of F^+ ions is expected to

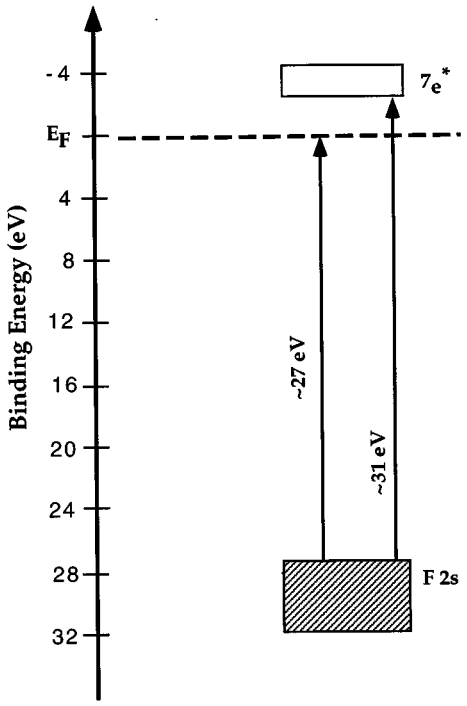

FIG. 10. Schematic drawing illustrating a possible near threshold ESD F^+ desorption mechanism from adsorbed PF_3 via an electronic excitation.

originate from the topmost PF_3 layers, the F^+ signal obtained from a thick PF_3 film (>2 ML PF_3 on PF_3) includes some contribution from the ions originating near the PF_3/Pt interface. When the PF_3 film is thicker the contribution from the ions desorbing near the PF_3/Pt interface becomes smaller. Hence, the influence of the Pt substrate on F^+ desorption from a very thick PF_3 film ($\geqslant$6 ML PF_3 on Pt) is expected to be negligible. As the PF_3 films become thicker, the electronic band structure of PF_3 becomes more bulklike. Since the electronic bands of the thick film ($\geqslant$5 ML of PF_3) are expected to be fully formed,[48] and electronic transition from the F $2s$ level to the lowest lying conduction band minimum (CBM) of the bulk PF_3 may become the dominant process in determining the F^+ desorption from the thick PF_3 films. (Note: As seen in Fig. 10, for chemisorbed PF_3, an electronic transition from the F $2s$ level to the antibonding $7e$ level is estimated to require a minimum of 31 eV.) We expect that the F $2s \rightarrow 7e$ transition in the condensed phase is different in energy from the gas phase value for two reasons. First, the bottom of the antibonding $7e$ band of the bulk PF_3 may be lower in energy than the $7e$ orbital energy of an isolated PF_3. Secondly, we expect that in the condensed phase the energy required for the F $2s \rightarrow 7e$ transition is lower by 0.7–1 eV due to the polarization force of the solid PF_3.[21,23] Therefore, it seems that the near threshold desorption of F^+ from the thick PF_3 layer may be initiated via electronic transitions from the F $2s$ level to the bottom of the antibonding $7e$ band of the bulk PF_3.

After an F $2s$ electron is promoted (by electron impact) to the Fermi level for the thin PF_3 films, or to the $7e$ band of the bulk PF_3 for the thick PF_3 films, decay-channels may be then opened for the relaxation of excess energy. The F^+ threshold for PF_3 on Pt may be due to the creation of 2H final states (highly repulsive) resulting from decay of the F $2s$ hole. As discussed above, there are some satellite 2h1e states above the $(\mathrm{F}\ 2s)^{-1}$ state, therefore, it is also possible that the $(\mathrm{F}\ 2s)^{-1}$ potential curve may cross the 2h1e potential energy curves at some internuclear separation. The curve crossing may lead to F^+ desorption via predissociation. However, in order to discuss these processes in more detail, the potential energy surfaces of PF_3 must be known.

In summary, one-electron valence ionization of PF_3 and dipolar dissociation of PF_3 cannot explain the observed F^+ desorption yield functions. However, an initial excitation from the F $2s$ orbital to the substrate Fermi level or to an unoccupied level in PF_3 may result in the desorption of F^+ ions near the observed threshold. The 2h1e (2-hole 1-electron) valence excitations lying near the $(\mathrm{F}\ 2s)^{-1}$ state may also be involved in the near threshold F^+ desorption from adsorbed PF_3 (1 ML PF_3/Pt).

Within the limits of our signal to noise, we do not observe a significant threshold at the P $2p$ excitation energy ~135 eV,[49] in contrast to PSD measurements of PF_3 on Ru(0001). The ESD F^+ yield at 135 eV contains contributions from ESD F^+ mechanisms having thresholds at all energies $\leqslant$135 eV. Since the excitation probability for core electron decreases strongly with increasing electron binding energy, the contribution of the ESD mechanism with the ~27 eV threshold to the ESD F^+ yield at 135 eV is expected to be considerably larger than the F^+ yield due to the P $2p$ excitation. Therefore, we believe that the contribution of the P $2p$ excitation to the F^+ ESD yield at $E(e)=135$ eV cannot be resolved.

C. Mechanisms of ESD of P^+ from adsorbed PF_3

As seen in Figs. 7 and 9, the ESD P^+ threshold energy from the thick PF_3-layer is ~23 eV. In the gas phase, the P^+ appearance potential from PF_3 under electron impact is 32.5 eV.[12] Consider the possibility that P^+ formation from PF_3 proceeds via the dissociative ionization (DI) reactions

$$e^- + \mathrm{PF_3} \rightarrow \mathrm{P^+} + 3\mathrm{F} + 2e^-, \tag{7}$$

$$e^- + \mathrm{PF_3} \rightarrow \mathrm{P^+} + \mathrm{F_2} + \mathrm{F} + 2e^-. \tag{8}$$

Taking $D(\mathrm{PF_3} \rightarrow \mathrm{P}+3\mathrm{F})=14.4$ eV and $D(\mathrm{PF_3} \rightarrow \mathrm{P}+\mathrm{F_2}+\mathrm{F}) \approx 12.8$ eV (dissociation energies),[43] and $I(\mathrm{P}) \approx 10.5$ eV (the ionization potential of P),[50] we estimate the thermodynamic threshold energy for zero kinetic energy P^+ to be ~24.9 eV for reaction (7) and ~23.3 eV for reaction (8). In ESD the electronic transition leading to desorption of energetic ions should be a few eV higher than the gas phase thermodynamic threshold value (~24.9 eV). Although in the condensed phase, the threshold energy is expected to be lower by 0.7–1 eV due to the induced polarization force,[21,23] the ESD threshold energies for reactions (7) and (8) are still expected to be larger than the observed ESD P^+ threshold energy (~23 eV). This indicates that the near threshold P^+

desorption does not appear to be possible via a DI reaction. As discussed in Sec. IV B 2, DD does not lead to the P^+ formation from the thick PF_3.

Another possible reaction pathway which could lead to P^+ production is the direct ionization of the $6a_1$ orbital. As seen in Table II, the ionization potential of the $6a_1$ orbital is ~22.8 eV with respect to the vacuum. Recently Ohno *et al.*[51] have calculated the valence photoemission spectra of PF_3 by using the *ab initio* diagrammatic construction [ADC(3)] Green's functional method. They have shown that following the ionization of the $6a_1$ orbital, the $(6a_1)^{-1}$ hole may decay to form either a $8a_1^{-2}9a_1^1$, 2h1e (2-hole 1-electron), final state or a $4e(5e \text{ and } 6e)^{-1}8a_1^{-1}7e^1$ (2h1e) final state. These final states are induced by the intraligand hole hopping dynamical relaxation. These final states may lead to desorption of a P^+ ion from absorbed PF_3. Therefore, we suggest that the $8a_1^{-2}9a_1^1$ and/or $4e(5e \text{ and } 6e)^{-1}8a_1^{-1}7e^1$ multivalence-hole final states that result from the decay of a $(6a_1)^{-1}$ hole may give rise to P^+ desorption from the condensed PF_3 layer.

D. Mechanisms of ESD of PF^+ from adsorbed PF_3

As seen in Fig. 9, the PF^+ threshold energy from the thick PF_3 is about 25 eV. In the gas phase, the threshold energy for the PF^+ formation from PF_3 have been found to be ~21 eV. In the gas phase, some possible dissociative ionization reactions which could lead to formation of PF^+ are

$$e^- + PF_3 \rightarrow PF^+ + F_2 + 2e^-, \tag{9}$$

$$e^- + PF_3 \rightarrow PF^+ + 2F + 2e^-. \tag{10}$$

We can determine the threshold energies for reactions (9) and (10) to be ~16.8 and ~19.5 eV, respectively.[12,43] Based on the above discussion, we think that both reactions are energetically possible in our experiment.

As discussed in Sec. IV B 2, we conclude that DD does not lead to the PF^+ formation from the thick PF_3. The PF^+ ion formation from adsorbed PF_3 may be initiated by ionization of the $6a_1$ orbital. As seen in Fig. 9, the PF^+ threshold energy is about 3 eV higher than the $6a_1$ ionization potential. One possibility for the PF^+ threshold energy shift is the influence of the polarization potential on the PF^+ desorption. The PF^+ generated under 23–25 eV electron impact may not be able to overcome the polarization potential to escape from the surface. This may cause a shift in the ion desorption threshold energy.

As seen in Fig. 9, both P^+ and PF^+ yield curves exhibit a change in slope near 32 eV, the region of the F^+ threshold. This observation suggests that the excitation of the F 2*s* level (such as 2h, 2h1e) leads to desorption of F^+, P^+, and PF^+ ions from PF_3 for electron energies above 32 eV. Multivalence hole final states resulted from the decay of the F 2*s* hole may determine the ion desorption intensities from PF_3. It is also possible that some 2h or 2h1e multivalence states may contribute to desorption of F^+, P^+, and PF^+ from a thick PF_3 film for electron energies above 32 eV, as discussed in Sec. IV B 3.

V. CONCLUSIONS

We have measured the ion yields, thresholds and kinetic energy distributions for electron stimulated desorption of F^+, P^+, and PF^+ ions from PF_3 adsorbed on a Pt surface. We have found that the threshold energy for F^+ desorption from adsorbed PF_3 depends on the PF_3 film thickness; the F^+ appearance potentials are ~26.5 eV from a 1 ML PF_3 on Pt surface and ~28.5 eV from a thick PF_3 film (6 ML PF_3) on Pt. The peak kinetic energy of F^+ is ~4 eV, independent of electron energies between 40 and 175 eV. The P^+ threshold energy from the thick PF_3 film is ~23 eV. The P^+ ions generated under 56 eV electron bombardment desorb with a peak energy of ~2 eV. The F^+ threshold for adsorbed PF_3 on the Pt is believed to be due to the excitation of the F 2*s* level. The near threshold P^+ formation can be correlated to the ionization of the $6a_1$ level. Beyond near threshold (>32 eV), the excitation of the F 2*s* level seems to play an important role in the desorption of P^+ and PF^+ ions from adsorbed PF_3. Our results indicate that neither one-electron valence ionization (dissociative ionization) nor dipolar dissociation processes seems to contribute the near threshold F^+ and P^+ desorption from adsorbed PF_3.

ACKNOWLEDGMENTS

This work has been supported in part by the US National Science Foundation (Grant No. CHE-9408367), and the Medical Research Council of Canada.

[1] T. E. Madey, S. A. Joyce, and A. L. Johnson, in *Interaction of Atoms and Molecules with Solid Surfaces*, edited by V. Bortolani, N. H. March, and M. P. Tosi (Plenum, New York, 1990), p. 459.
[2] A. L. Johnson, S. A. Joyce, and T. E. Madey, Phys. Rev. Lett. **61**, 2578 (1988).
[3] S. A. Joyce, C. Clark, V. Chakarian, D. K. Shuh, J. A. Yarmoff, T. E. Madey, P. Nordlander, B. L. Maschhoff, and H. S. Tao, Phys. Rev. B **45**, 14264 (1992).
[4] J. T. Yates, Jr., M. D. Alvey, M. J. Dresser, M. A. Henderson, M. Kiskinova, R. D. Ramsier and A. Szabó, Science **255**, 1397 (1992).
[5] R. D. Ramsier, and J. T. Yates, Jr., Surf. Sci. Rep. **12**, 243 (1991).
[6] N. J. Sack and T. E. Madey, Surf. Sci. **347**, 367 (1996).
[7] M. D. Alvey, J. T. Yates, Jr., and K. J. Uram, J. Chem. Phys. **87**, 7221 (1987).
[8] M. D. Alvey and J. T. Yates, Jr., J. Amer. Chem. Soc. **110**, 1782 (1988).
[9] R. E. Johnson, *Energetic Charged Particle Interactions with Atmospheres and Surfaces*, Physics and Chemistry in Space (Springer, Berlin, 1990).
[10] K. A. G. MacNeil and J. C. J. Thynne, J. Chem. Phys. **74**, 2257 (1970).
[11] P. W. Harland, D. W. H. Rankin, and J. C. J. Thynne, Int. J. Mass Spectrum. Ion Phys. **13**, 395 (1974).
[12] D. F. Torgerson and J. Westmore, Can. J. Chem. **53**, 933 (1975).
[13] M. Akbulut, T. E. Madey, L. Parenteau, and L. Sanche, J. Chem. Phys. **105**, 6043 (1996), following paper.
[14] N. J. Sack, M. Akbulut, and T. E. Madey, Surf. Sci. Lett. **334**, L695 (1995).
[15] T. E. Madey, N. J. Sack, and M. Akbulut, Nucl. Instrum. Methods Phys. Res. B **100**, 309 (1995).
[16] M. Akbulut, N. J. Sack, and T. E. Madey, Phys. Rev. Lett. **75**, 3414 (1995).
[17] F. Nitschké, G. Ertl, and J. Küppers, J. Chem. Phys. **74**, (1981).
[18] M. A. Huels, L. Parenteau, M. Michaud, and L. Sanche, Phys. Rev. A **51**, 337 (1995).
[19] L. Parenteau, J.-P. Jay-Gerin, and L. Sanche, J. Phys. Chem. **98**, 10277 (1994).
[20] P. Rowntree, L. Parenteau, and L. Sanche, J. Chem. Phys. **94**, 8570 (1991).

[21] M. A. Huels, L. Parenteau, and L. Sanche, J. Chem. Phys. **100**, 3940 (1994).
[22] P. Rowntree, L. Sanche, and L. Parenteau, J. Chem. Phys. **101**, 4248 (1994).
[23] L. Sanche, in *Linking the Gaseous and Condensed Phases of Matter*, edited by L. G. Christophorou, E. Illenberger, and W. F. Schmidt (Plenum, New York, 1994) p. 31.
[24] L. Sanche, in *Excess Electrons in Dielectric Media*, edited by C. Ferradini and J.-P. Jay-Gerin (CRC, Boca Raton, FL, 1991), p. 1.
[25] P. Avouris and R. E. Walkup, Annu. Rev. Phys. Chem. **40**, 173 (1989).
[26] M. L. Knotek, Rep. Prog. Phys. **47**, 1499 (1984).
[27] T. E. Madey, Science **234**, 316 (1986).
[28] H. Sambe, D. E. Ramaker, L. Larenteau, and L. Lanche, Phys. Rev. Lett. **59**, 236 (1987).
[29] D. Menzel, Nucl. Instrum. Methods Phys. Res. Sect. B **13**, 507 (1986).
[30] T. E. Madey, R. Stockbauer, S. A. Flodström, J. F. v.d. Veen, F. J. Himpsel, and D. E. Eastman, Phys. Rev. B **23**, 6847 (1981).
[31] J. A. Kelber and M. L. Knotek, Surf. Sci. **121**, L499 (1982).
[32] J. A. Kelber and M. L. Knotek, J. Vac. Sci. Technol. A **1**, 1149 (1983).
[33] J. A. Kelber and M. L. Knotek, Phys. Rev. B **30**, 400 (1984).
[34] D. E. Ramaker, J. Chem. Phys. **78**, 2998 (1983).
[35] D. E. Ramaker, Chem. Phys. **80**, 183 (1983).
[36] T. E. Madey, D. E. Ramaker, and R. Stockbauer, Annu. Rev. Phys. Chem. **35**, 215 (1984).
[37] M. L. Knotek and P. J. Feibelman, Phys. Rev. Lett. **40**, 964 (1978).
[38] L. Sanche, Scanning Microscopy **9**, 619 (1996).
[39] M. Akbulut and T. E. Madey (in preparation).
[40] S.-X. Xiao, W. C. Trogler, D. E. Ellis, and Z. Berkovitch-Yellin, J. Am. Chem. Soc. **105**, 7033 (1983).
[41] V. Chakarian, D. K. Shuh, J. A. Yarmoff, H.-S. Tao, U. Diebold, B. L. Maschhoff, and T. E. Madey, J. Chem. Phys. **100**, 5301 (1994).
[42] J. Hölzl and F. K. Schulte, in *Solid Surface Physics*, edited by G. Höhler (Springer, Berlin, 1979), p. 1.
[43] G. L. Gutsev, J. Chem. Phys. **98**, 444 (1993).
[44] R. Franchy and D. Menzel, Phys. Rev. Lett. **40**, 964 (1979).
[45] J. A. Yarmoff, D. K. Shuh, V. Chakarian, T. D. Durbin, K. A. H. German, and C. W. Lo, in *Desorption Induced by Electron Transitions DIET V*, edited by A. R. Burns, E. B. Stechel, and D. R. Jennison (Springer, Berlin, 1993), p. 253.
[46] K. Miura, K. Sugiura, and H. Sugiura, Surf. Sci. Lett. **253**, L407 (1991).
[47] M. J. Bozack M. J. Dresser, W. J. Choyke, P. A. Taylor, and J. T. Yates Jr., Surf. Sci. Lett. **184**, L332 (1987).
[48] R. A. Heaton and C. C. Lin, Phys. Rev. B **22**, 3629 (1980).
[49] S. A. Joyce, J. A. Yarmoff, and T. E. Madey, Surf. Sci. **254**, 144 (1991).
[50] E. W. McDaniel, *Atomic Collisions: Electron and Photon Projectiles* (Wiley, New York, 1989).
[51] M. Ohno, W. v. Niessen, and V. Zakrzewski, J. Chem. Phys. **97**, 6953 (1992).